# Land Cover and Climate Change Impact on River Discharge: Case Study of Upper Citarum River Basin

**Arno Adi Kuntoro*, Muhammad Cahyono & Edy Anto Soentoro**

Faculty of Civil Engineering and Environment, Institut Teknologi Bandung,
Jalan Ganesha 10, Bandung 41032, Indonesia
*E-mail: arnoak@ftsl.itb.ac.id

**Abstract.** The Upper Citarum River Basin is the main catchment area of the Saguling Dam, the most upstream of three cascade dams in the Citarum River Basin. During the last 30 years, rapid economic development has led to an increase of water extraction and land conversion from green area to developed area. Also, evidence of climate change can clearly be seen from the climatological records of a number of climatology stations in this basin over the last few decades. In this study, the effect of anthropogenic and climate change in the Upper Citarum River Basin river discharge was simulated using the Sacramento Catchment Model. Historical river discharge, rainfall, climatology, and land cover from 1995 to 2009 were used for model calibration and verification. The multi-model mean monthly rainfall and the temperature projection taken from Coupled Model Intercomparison Project 5 (CMIP5) for the RCP6 and RCP8.5 climate change scenarios were statistically downscaled and used as input for a simulation of future river discharge from 2030 to 2050. The result showed that the combination of anthropogenic and climate change may result in a significant decrease of low flow in the Upper Citarum River Basin. This study underlines the importance of land cover and climate change factors for future infrastructure planning and management in the Upper Citarum River Basin.

**Keywords:** *Citarum River Basin; climate change; CMIP5; land cover change; river discharge; Sacramento Catchment Model.*

## 1 Introduction

The Citarum River Basin (CRB) is one of the most important river basins for West Java Province and the Special Region of Jakarta. To have a reliable water supply for domestic, agriculture, and energy use in the surrounding area, three cascade dams have been built along the main Citarum river: Saguling, Cirata, and Jatiluhur. About 240 thousand hectares of irrigation area rely on water supply from Jatiluhur Dam. Yet, the area downstream of the cascade dams still experiences floods in extremely wet years (for example in 2010) and droughts in extremely dry years (for example in 2015).

Received April 18th, 2018, Revised August 13th, 2018, Accepted for publication August 13th, 2018.
 ISSN: 2337-5779, DOI: 10.5614/j.eng.technol.sci.2018.50.3.4

The Upper CRB is the main catchment area of the Saguling Dam, the most upstream dam of the three cascade dams. The Upper CRB covers a number of districts, including Bandung city, where floods occur almost annually. High sedimentation and riverbank acquisition, mostly for settlement, have reduced channel capacity to convey flood discharge. Furthermore, the flat topographical conditions in the middle of the Upper CRB results in relatively long periods of inundation during flooding [1].

During the last 30 years, this basin has experienced rapid economic development, which has led to an increase of water extraction and land conversion from green or conservation area to open or developed area. Water demand has increased because of high population growth in more densely populated areas, economic development, and a higher life standard, leading to increased extraction of surface water and ground water [2-4]. Prolonged droughts, as affected by climate change, may disturb agricultural production in Indonesia, including in the CRB area. Water scarcity during the dry season could result in more severe conflicts and competition among water users [5].

Indonesia is influenced by the Indian Ocean Dipole (IOD) and El-Niño Southern Oscillation (ENSO). The Western part of Indonesia is affected mostly by IOD, while the Eastern part is mostly affected by IOD. Being located between two oceans, climate variability has a significant impact on the Indonesian climate. The Upper CRB is located on Java Island in the middle of the Indonesia archipelago and therefore climate variability in the Indian and Pacific Ocean have a significant impact on river discharge in the Upper CRB [6,7].

Historical records of river discharge in the Upper CRB for the last decades show that although the annual average discharge is relatively constant, the average river discharge in the wet season shows an increasing trend, while the average river discharge in the dry season shows a decreasing trend. Historical records of monthly rainfall display a similar pattern: although the annual average rainfall is relatively constant, the average monthly rainfall in the wet season shows an increasing trend, while the average monthly rainfall in the dry season shows a decreasing trend. Both river discharge and rainfall data records indicate that human activities and climate change could contribute to more intense floods and droughts in the future [1].

The water resource problem in the Upper CRB is an example of a case where flood and drought cannot be solved only by infrastructure development. Good land use and water resources management, adequate infrastructure maintenance and operations, climate prediction, hazard mitigation and information

dissemination are necessary to minimize the impact of water-related hazards in the future [8].

## 2 Materials and Method

### 2.1 Location of Study Area, Historical Rainfall, Land Cover Change

The Upper CRB is located between 107°10' and 108°00' East and between 6°40' and 7°20' South, covering an area of about 1700 km$^2$. Administratively, it covers the area of West Bandung Regency, Bandung Regency, Bandung city, Cimahi city, and Sumedang Regency. The Upper CRB consists of 13 river sub-catchments: Citarum Hulu, Citarik, Cikeruh, Cikapundung, Cisangkuy, Cipamokolan, Cidurian, Cicadas, Citepus, Cisangkuy, Cibolerang, Ciwidey and Cibereum rivers, which flow toward the main stream of the Citarum river in the middle of the Upper CRB. The Nanjung River Discharge Station is located downstream of the CRB, before the Citarum river flows into the Saguling Dam. In this study, Nanjung Station delineates the downstream boundary of the Upper CRB catchment. The location of the Upper CRB is shown in Figure 1.

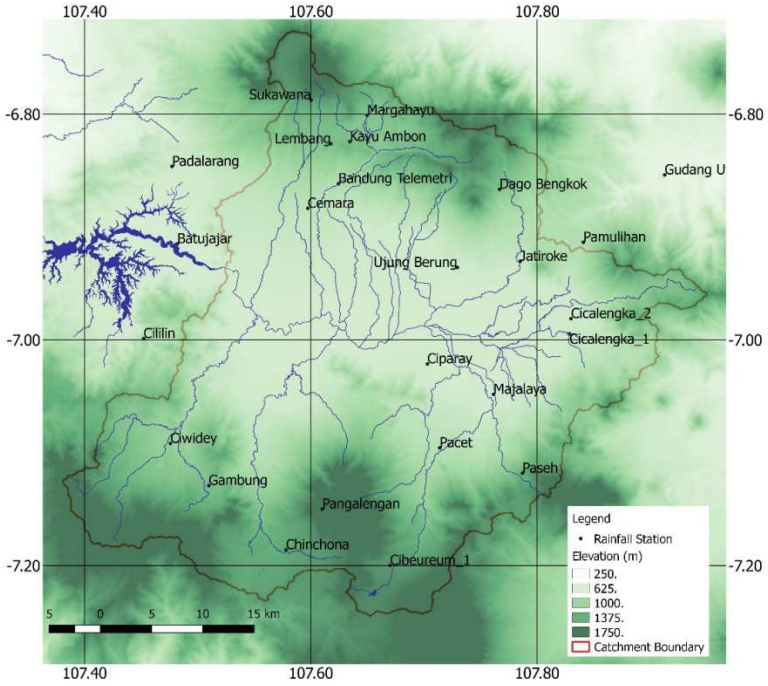


**Figure 1** Location of study area.

A Thiessen polygon was used to compute the catchment rainfall average in the Upper CRB for 26 rainfall stations (see Figure 1). Based on computation using the Thiessen method, the average rainfall in the Upper CRB from 1980 to 2009 was 1892 mm/year, varying from a minimum of 1356 mm/year in 1982 to a maximum of 2523 mm/year in 1986. Average monthly rainfall in the rainy season (October-March) and the dry season (April-September) was 77 mm/month and 243 mm/month, respectively.

A time series of Google Earth images of the Upper CRB, dated 1985, 1995, 2005 and 2015, shows the trend of increasing developed area and moderately vegetated area and decreasing highly vegetated area. A rough projection of land cover change based on these images shows that within 30 years highly vegetated area will decrease from 37.1% to 19.4% coverage, moderately vegetated area will increase from 52.4% to 57.5% coverage, while the total of moderately and highly developed area will increase from 10.5% to 23.1%. An indication of land cover change in the Upper CRB is shown in Figure 2.

Figure 2 shows that the trend of land cover change is relatively linear, especially for moderately developed area ($r^2$ = 0.994). Therefore, a linear trend of land cover change was assumed in making a projection of future land cover.

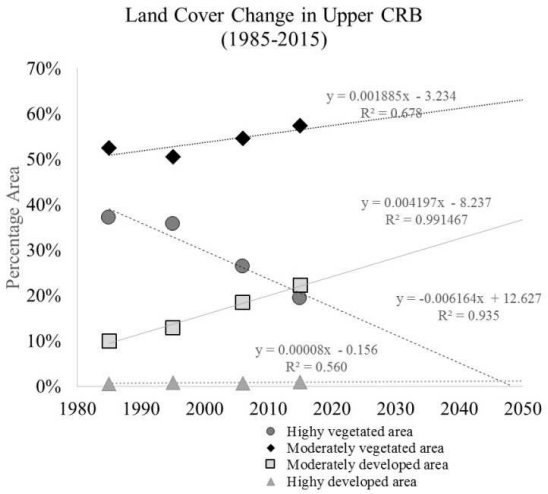


**Figure 2** Trend of land cover change in the Upper CRB.

## 2.2 Future Climate Projection

The World Climate Research Program (WCRP) Working Group on Coupled Modelling (WGCM) started promoting the fifth phase of the Coupled Model Inter-comparison Project (CMIP5) in 2008. The objective of CMIP5 is to

provide a framework for coordinated climate change experiments for assessment within the scope of AR5 and beyond.

Average monthly rainfall and temperature from the multi-model mean of CMIP5 results for climate change scenarios RCP6 and RPC8.5 were used as data input in a rainfall-runoff model for projecting the future discharge in the Upper CRB. The CMIP5 dataset covers the result of 39 scenario runs from different models. The data were downloaded from KNMI Climate Explorer website [9] (https://climexp.knmi.nl).

## 2.3 Statistical Downscaling of Future Rainfall Projection

Downscaling is a method for obtaining high-resolution climate information from relatively coarse global climate models (GCMs). The spatial resolution of the CMIP5 datasets is about 2.5° x 2.5° (275 x 275 km near the equator), which is far greater than the area of the Upper CRB, which is only about 50 x 40 km. Therefore, a downscaling method was applied to correct the large-grid CMIP5 dataset for the smaller grid of the Upper CRB.

Many studies have used statistical downscaling techniques for basin scale hydrology analysis. For example, [10] used four statistical downscaling methods to get 12-km grid resolution data from the original NCEP/NCAR Reanalysis grid size, to simulate wet-day fraction, extreme events, and weather patterns in the United States. Reference [11] used three statistical downscaling methods for simulating trends of wet spell, dry spell, and rainfall inter-annual variability in the Yellow River Region. Reference [12] used fifteen different RCP models and several statistical downscaling methods to simulate extreme river flows in 11 catchments in the European region. Reference [13] used statistically downscaled GCM output to simulate river discharge in the Upper Hanjiang Basin, China. Reference [14] used a statistical bias correction method for extreme rainfall, normal rainfall and frequency of dry days. Bias correction of heavy rainfall was conducted by using generalized Pareto distribution (GPD), while bias correction of normal rainfall was conducted by using monthly correction and frequency based on gamma distribution.

Since the output of CMIP5 is in the form of a monthly series, a stochastic approach is needed to generate daily precipitation series from the monthly data. Similar approaches have been used in other studies. For example, [15] generated correlated daily rainfall by using a diagonal band copula with a single parameter to generate lag-1 correlated random numbers for application in case studies of Parafield, South Australia and Mesing, Malaysia. Reference [16] used a 10-state first-order Markov chain and a non-parametric rainfall model,

adopting a doubly-stochastic transition-matrix, for application in a case study of the Torne River Catchment, Northern-Sweden/Western-Finland.

The present study combines the concept of statistical downscaling used by [14] and the stochastic method used by [15] to generate daily rainfall series for future scenarios based on monthly rainfall projections from CMIP5. Computation steps for this analysis were as follows: 1) develop correction functions for CMIP5 rainfall data for the historical time series (1980-2009); 2) apply the correction functions from step 1 to CMIP5 future rainfall projections (2030-2050); 3) generate daily rainfall series from the corrected monthly data in step 2 based on the daily rainfall probability curve for 5 monthly rainfall categories: dry, normal-dry, normal, normal-wet, and wet.

In the first step, historical monthly rainfall records from 1980 to 2009 were plotted together with the CMIP5 multi-model mean for the same period. Correction functions were applied to match the multi-model mean rainfall probability distribution curve with historical rainfall distribution in the Upper CRB. The rainfall data correction functions that gave the smallest error compared to the historical dataset were in Eqs. (1) and (2):

$$C_1 = -0.1273 \ln (P) + 0.6726 \ \{0 \leq P < 0.6\} \quad (1)$$

$$C_2 = -1.7844 (P) + 1.8099 \ \{P \geq 0.6\} \quad (2)$$

where $C_1$ and $C_2$ are CMIP5 rainfall data correction factors, and P is probability of occurrence. The plot of historical rainfall data, CMIP5 mean rainfall data, and the corrected CMIP5 data are shown in Figure 3.

In the second step, a stochastic approach was used to generate daily rainfall series from the corrected CMIP5 monthly data as in Eqs. (3) to (7) as follow:

$$prob_{month} = \frac{n_{rain}}{n_{day}} \quad (3)$$

$$x = rand(0 - 1) \quad (4)$$

$$rain_{day} = \begin{cases} \gamma^{-1}(\alpha, \beta, x); for\ x < prob_{month} \\ 0; for\ x \geq prob_{month} \end{cases} \quad (5)$$

$$rain_{month}{}' = \sum_{d=1}^{n_{day}} rain_{day} \quad (6)$$

$$rain_{day}{}' = rain_{day} \frac{rain_{month}}{rain_{month}{}'} \quad (7)$$

where:

$prob_{month}$ is the probability of occurrence of rainfall in a month, $x$ is a random number between 0 and 1, $n_{rain}$ is the average number of rain days in a month,

$n_{day}$ is the number of days in a month, $\gamma^{-1}(\alpha,\beta,x)$ is the inverse gamma distribution of daily rainfall in the Upper CRB: $rain_{month}'$ is the sum of daily rainfall, $rain_{day}$ is the daily rainfall computed from Eq. (5), $rain_{day}'$ is the normalized daily rainfall, and $rain_{month}$ is the actual monthly rainfall.

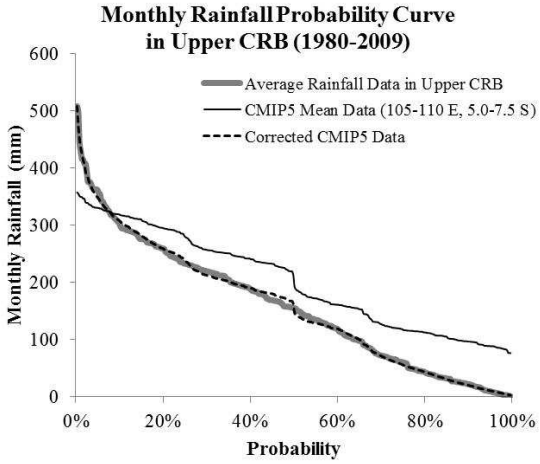


**Figure 3** Historical, CMIP5, and corrected CMIP5 rainfall data for the Upper CRB.

Two approaches were used to represent the daily rainfall distribution function: 1) using two categories of monthly rainfall, i.e. below average months ($R < R_{50\%}$) and above average months ($R > R_{50\%}$); 2) using five categories of monthly rainfall, i.e. dry months ($R < R_{80\%}$); dry-normal months ($R_{80\%} \leq R < R_{60\%}$); normal months ($R_{60\%} \leq R < R_{40\%}$); wet-normal months ($R_{40\%} \leq R < R_{20\%}$); and wet months ($R \geq R_{20\%}$).

The values of $\alpha$ and $\beta$ in gamma distribution for each rainfall category are shown in Table 1.

**Table 1** Values of α and β in Gamma distribution for monthly rainfall series.

| Category of monthly rainfall | α | β |
|---|---|---|
| Below average ($R < R_{50\%}$) | 0.636 | 5.674 |
| Above average ($R \geq R_{50\%}$) | 1.348 | 6.405 |
| Wet ($R \leq R_{20\%}$) | 1.549 | 6.801 |
| Normal-wet ($R_{20\%} < R \leq R_{40\%}$) | 1.273 | 5.689 |
| Normal ($R_{40\%} < R \leq R_{60\%}$) | 0.869 | 5.785 |
| Normal-dry ($R_{60\%} < R \leq R_{80\%}$) | 0.465 | 5.399 |
| Dry ($R \leq R_{80\%}$) | 0.119 | 5.501 |

### 2.3.1 Catchment Average Temperature

Data from four climatology stations in West Java (Bandung, Citeko, Darmaga, and Jatiwangi) were used to correct the CMIP5 multi-model mean average temperature data for the Upper CRB catchment. The average temperature was assumed to be correlated linearly to ground elevation. The average temperature data from the above stations are shown in Figure 4. The trend line for obtaining the average temperature from the given ground elevation is as in Eq. (8).

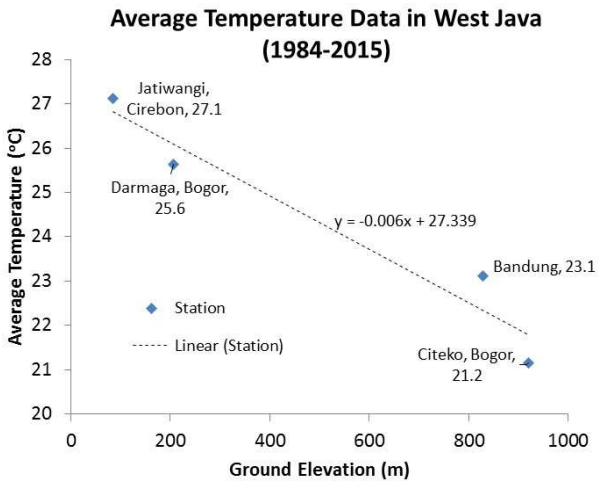


**Figure 4** Average temperature data for West Java.

$$T = 27.34 - 0.006H \tag{8}$$

where T is the average temperature, and H is the ground elevation from mean sea level (m).

For daily rainfall-runoff simulation, linear interpolation was used to generate a daily temperature series from the monthly data by assuming that the average monthly temperature occurs in the middle of each month.

### 2.3.2 Catchment Average Evapotranspiration

The Thornthwaite method was used to estimate the average evapotranspiration for the Upper CRB. While other evapotranspiration calculation methods use several climatology parameters, such as wind speed, humidity and sunshine duration, Thornthwaite's method only uses temperature data, which are available in most GCM datasets, including CMIP5.

### 2.3.3 Rainfall-runoff Model

This study used the Sacramento Catchment Model to simulate river discharge from rainfall and evapotranspiration input. The Sacramento Catchment Model was developed in the 1970s for the California-Nevada River Forecast System to provide an effective technique for streamflow forecasting. This model uses precipitation, evapotranspiration, and a number of catchment characteristics as input for the discharge computation by considering hydrological processes such as soil moisture, water balance, direct runoff, surface runoff, interflow, and base flow [17,18]. After more than 40 years, this model is still widely used in hydrological research all over the world. For example, [19] used the Sacramento model together with two other rainfall runoff models to simulate current and future discharge in the Upper Niger Basin; [20] used the Sacramento model together with four other rainfall runoff models to simulate streamflow in the Molawin and Eastern Dampalit Watershed in the Philippines; [21] coupled the Snow-17 model with the Sacramento model to simulate hydrological response in 671 river basins in the United States.

To include the effect of land cover change in the rainfall-runoff model, historical river discharge, rainfall, and temperature data from 1995 to 1999 were used for model calibration for the early years of catchment condition, while historical data from 2005 to 2009 were used for model calibration in later years of catchment condition. Nash Sutcliffe Efficiency (NSE) and Correlation Coefficient ($r^2$) were used as statistical indicators of goodness-of-fit between the model and the data.

For the future scenario, the corrected CMIP5 multi-model mean of the rainfall and temperature datasets from 2030 to 2050 was used as input for the rainfall-runoff model. Two scenarios of future change were applied: the first by assuming the same impervious land cover in 2030-2050 as indicated by the land cover map from 2015; the second by assuming a linear trend of increase of impervious land cover in the future based on land cover change from 1980 to 2015.

## 3 Results and Discussion

### 3.1 Rainfall-runoff Model Calibration

Calibration was conducted by adjusting several main parameters that represent hydrological characteristics in the Sacramento Catchment Model. The used values based on calibration from 1995-1999 and 2005-2009 are shown in Table 2. The calibration result is shown in a time series and flow duration curve between historical and simulated discharge in Figure 5.

**Table 2** Calibrated parameters for rainfall-runoff simulation.

| Parameters | Unit | Description | Value |
|---|---|---|---|
| UZTWM | mm | Upper zone tension water maximum | 75 |
| UZFWM | mm | Upper zone free water maximum | 100 |
| LZTWM | mm | Lower zone tension water maximum | 100 |
| LZFSM | mm | Lower zone secondary free water maximum | 5 |
| LZFPM | mm | Lower zone primary free water maximum | 5 |
| UZK | - | Upper zone coefficient | 0.03 or 0.1 |
| LZSK | - | Lower zone secondary coefficient | 0.03 |
| LZPK | - | Lower zone primary coefficient | 0.03 |
| ZPERC | - | Coefficient of percolation rate increase | 1 |
| REXP | - | Exponent of percolation rate | 3.0 |
| PFREE | - | Portion of percolated free water | 0.2 |
| PCTIM | - | Portion of impervious land area | 0.17-0.3* |

* PCTIM value for simulation of 1995-1999 = 0.29, and for 2005-2009 = 0.34

The NSE value ranges from -∞ to 1, where an NSE value of 1 represents a perfectly fitting model [22]. In general, a model with NSE > 0.5 is considered good. From the calibration process, it was found that UZK is the most sensitive parameter determining discharge fluctuation.

Two calibration sets were used by applying different values of UZK. Calibration 1 used a UZK value of 0.03, while Calibration 2 used a UZK value of 0.1. The result shows that Calibration 1 gave a relatively close result for low flow but underestimated high flow. Calibration 2 gave a relatively close result for high flow but underestimated low flow. Calibration 2 also gave a flat trend for low flow below $Q_{80\%}$. The calibration results for both sets are shown in Table 3.

**Table 3** Calibrated parameters for rainfall-runoff simulation.

| Year | UZK | NSE |
|---|---|---|
| 1995-1999 | 0.03 | 0.87 |
| 1995-1999 | 0.10 | 0.46 |
| 2005-2009 | 0.03 | 0.84 |
| 2005-2009 | 0.10 | 0.84 |

Compared to the goodness-of-fit criteria of NSE, both calibration results showed an acceptable to good result. Since the main purpose of this study was to analyze the trend of low flow, a UZK value of 0.3 was selected. The calibrated parameters were used to simulate river discharge trends by using climatological projection data as input under assumption of future land cover change.

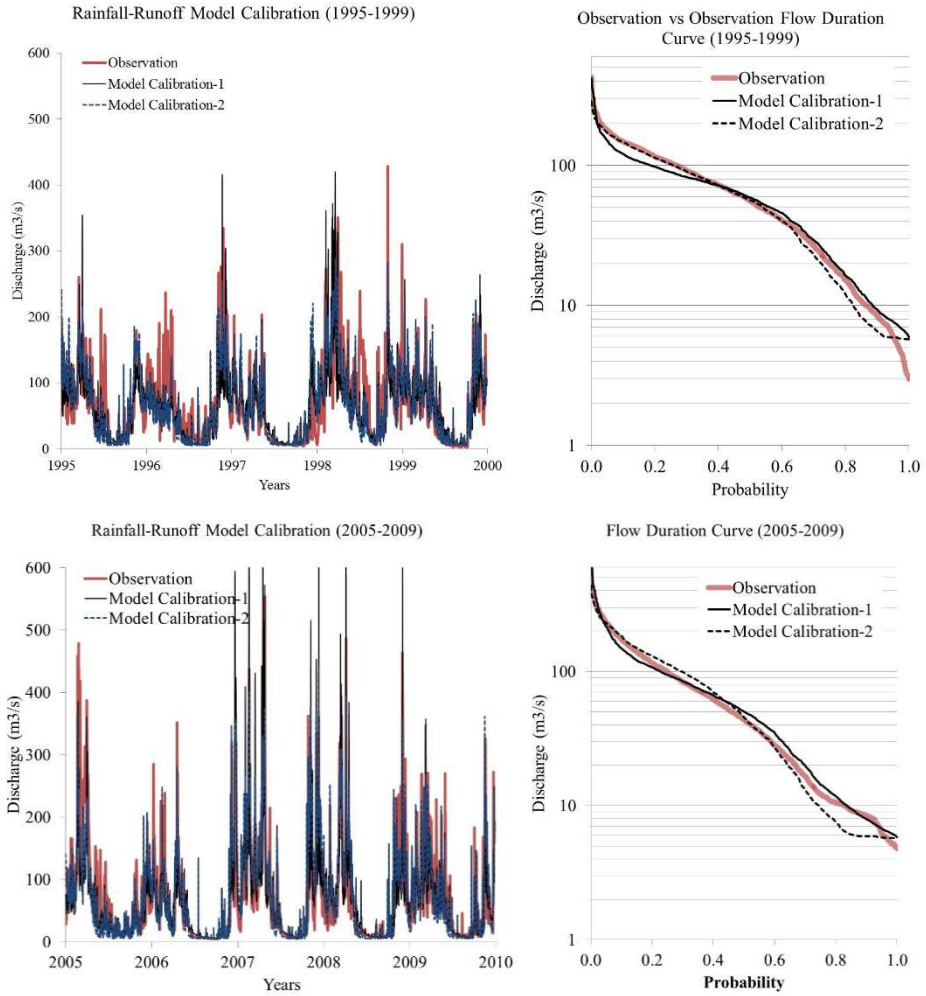


**Figure 5** Simulated vs. observed river discharge data for the Upper CRB.

## 3.2 Reliability of Stochastic Analysis for Daily Rainfall Generator

As previously described in Section 2.1.5, two approaches were used in the stochastic analysis for the daily rainfall generator: 1) using two categories of monthly rainfall, i.e. below average months ($R < R_{50\%}$) and above average months ($R > R_{50\%}$); 2) using five categories of monthly rainfall, i.e. dry months ($R < R_{80\%}$); dry-normal months ($R_{80\%} \leq R < R_{60\%}$); normal months ($R_{60\%} \leq R < R_{40\%}$); wet-normal months ($R_{40\%} \leq R < R_{20\%}$); and wet months ($R \geq R_{20\%}$). The rainfall probability curve of the historical rainfall data (1980-2009) while the stochastic data are shown in Figure 6.

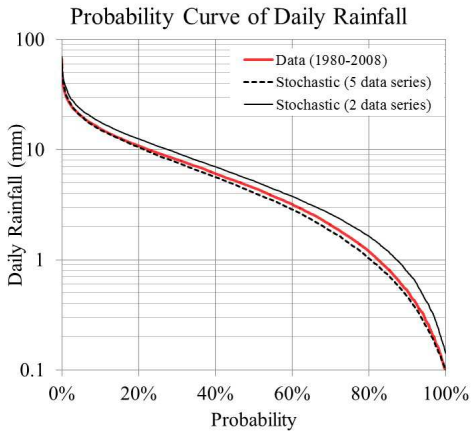


**Figure 6** Simulated vs. observed river discharge data for the Upper CRB.

Figure 6 shows that the use of five monthly rainfall categories for developing five gamma distribution functions gave relatively better results for the stochastic daily rainfall data. Meanwhile, the use of two gamma distribution functions gave overestimated results, the use of five gamma distribution function gave slightly underestimated results but they were closer to the data trend, especially at low flow. A comparison between the daily rainfall data and the stochastic data is shown in Table 4. From the comparison, the average deviation of the generated daily rainfall by using 5 functions compared with the historical data at extremely high rainfall ($R \geq R_{20\%}$) was about 0.2mm, while for extreme low rainfall ($R < R_{80\%}$) it was about 0.1 mm.

**Table 4** Calibrated parameters for rainfall-runoff simulation.

| Rainfall category | Average Rainfall Data (1980-2009) | Average of 2 Stochastic Functions | Average of 5 Stochastic Functions |
|---|---|---|---|
| $R \geq R_{20\%}$ | 17.6±6.8 mm | 20.3±8.0 | 17.4±7.0 |
| $R_{40\%} \leq R < R_{20\%}$ | 8.2±1.3 mm | 9.4±1.6 | 7.7±1.4 |
| $R_{60\%} \leq R < R_{40\%}$ | 4.5±0.8 mm | 5.2±0.9 | 4.1±0.8 |
| $R_{80\%} \leq R < R_{60\%}$ | 2.1±0.6 mm | 2.5±0.6 | 1.9±0.5 |
| $R < R_{80\%}$ | 0.6±0.3 mm | 0.7±0.5 | 0.5±0.3 |

The Kolmogorov-Smirnov (K-S) test was applied to test the reliability of the generated daily data compared to the historical data. By using $\alpha = 0.05$ for 199 samples, the maximum allowable deviation ($D_n^{\alpha}$) was 0.096. The maximum deviation for 2 and 5 stochastic functions was 0.048 and 0.032 respectively. The above analysis shows that the generated daily rainfall data were within the acceptable limit of error and could be used for further simulation.

### 3.3 Simulation of Future River Discharge Trends

For simulation of future river discharge trends, two scenarios were used: 1) considering climate change only; 2) considering climate change and land use change. For the first scenario, rainfall and temperature data from the corrected CMIP5 datasets were used and the proportion of impervious land cover in 2030-2050 was assumed to be similar with the proportion of impervious land cover in 2005. For the second scenario, the corrected climate change projection scenario data were used together with the assumption of a linear increase of the proportion of impervious land cover in 2030-2050. Estimation of impervious land cover was conducted by using the concept of composite runoff coefficient with the rational method. The assumed runoff coefficients for each land cover type and projection of impervious land cover in the Upper CRB are shown in Table 5.

**Table 5** Calibrated parameters for rainfall-runoff simulation.

| Year | HV | MV | MD | HD | C-composite |
|---|---|---|---|---|---|
| | C = 0.1 | C = 0.3 | C = 0.75 | C = 0.9 | (impervious cover) |
| 1985 | 37.1% | 52.4% | 9.9% | 0.6% | 0.274 |
| 1995 | 35.8% | 50.5% | 12.9% | 0.8% | 0.292 |
| 2005 | 26.3% | 54.5% | 18.5% | 0.7% | 0.335 |
| 2015 | 19.4% | 57.5% | 22.2% | 0.9% | 0.366 |
| 2045 | 2.2% | 62.5% | 34.7% | 1.2% | 0.460 |

Notes: HV = highly vegetated area; MV = moderately vegetated area; MD = moderately developed area; HD = highly developed area

Therefore, for Scenario 1, the proportion of impervious cover was about 0.34, i.e. the C-composite value in 2005. For Scenario 2, the proportion of impervious cover was about 0.46, which is the projection of C-composite in 2045. The simulation results of the above scenarios are shown in Figure 7.

Figure 7 shows that simulation with a land use change scenario tended to have higher high flow, which represents flood discharge, and lower low flow, which represents base flow during the dry season. The simulation result tended to be overestimated at very low flow (below Q90%). The historical data show a low flow decrease with a steeper trend, up to near-zero discharge, while the simulation result shows a milder trend, with minimum discharge about 5-6 $m^3/s$. Based on this comparison, the simulation result seems relatively valid up to $Q_{80\%}$. Therefore, analysis of the low flow trend was conducted by comparing the average low flow discharge with 80% probability of occurrence ($Q_{80\%}$).

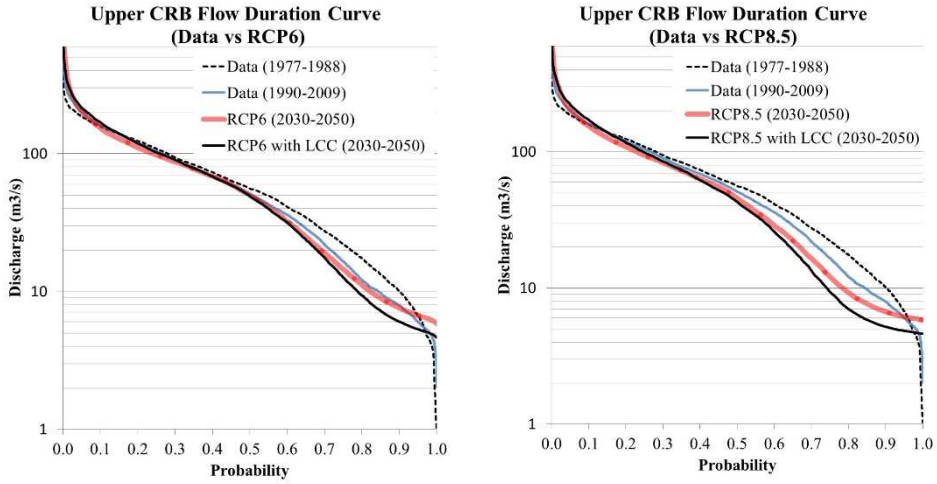


**Figure 7** Simulated river discharge data in the Upper CRB (2045-2050).

Q80% for 1977-1988 was about 17.5m$^3$/s, while it was about 11.2m$^3$/s for 1990-2009. The above comparison shows that within about 30 years, the historical data show a trend of Q80% decreasing in the Upper CRB by about 36%. For 'without land use change' in the RCP6 scenario, the projected $Q_{80\%}$ discharge in 2030-2050 is about 11.5 m$^3$/s. For 'with land use change scenario' in the RCP8.5 scenario, the projected $Q_{80\%}$ discharge in 2030-2050 is about 9.6m$^3$/s. The Q80% decrease for the RCP6 simulation compared to the period of 1997-1988 is 34.2% for the scenario without land use change and 45.1% for the scenario with land use change. For 'without land use change' in the RCP8.5 scenario, the projected $Q_{80\%}$ discharge for 2030-2050 is about 9.4 m$^3$/s, while for 'with land use change' in scenario RCP8.5, the projected $Q_{80\%}$ discharge in 2030-2050 is about 7.2m$^3$/s. The Q80% decrease for the RCP8.5 simulation compared to the period 1997-1988 is 46.3% without land use change and 58.9% with land use change.

The above simulations show that climate change leading to a decreasing trend of low flow in the Upper CRB is significant, even if land use change from pervious to impervious land cover is controlled or restrained to remain constant. From the historical land cover map of the Upper CRB it is likely that land use change to more impervious land cover will continue. It is very likely that the combination of climate change and land use change in the Upper CRB will result in more severe droughts in the future as well as more intense flooding. Therefore, an updated standard design for flood infrastructure, which covers the increasing trend of hydrological extremes, needs to be promoted in the future.

Population increase and economic growth will generate higher water demand. In the future, it is very likely that the water resources supply system in the Upper CRB will experience higher pressure due to the decreasing water availability as affected by climate change and land use change, and increasing water demand as affected by population increase and economic growth. Application of rainwater harvesting and water conservation by the community need to be promoted and disseminated to reduce the pressure on the existing public water supply system.

## 4 Conclusions

Historical data and simulation results on the Upper CRB show that the average low flow discharge ($Q_{80\%}$) tended to decrease from about 17.5$m^3$/s in 1977-1988 to about 11.2$m^3$/s in 1990-2009. Our simulation result for 2030-2050 shows that the low flow trend may continue to decrease in the future. Simulation by using the output of the multi-model mean of CMIP5 for RCP6 and RCP8.5 shows that Q80% in 2030-2050 may continue to decrease to about 11.5-9.4$m^3$/s, i.e. a decrease of 34.3-46.3% compared to the condition in 1977-1988. If the trend of land use change is included, Q80% in 2030-2050 could be even lower at about 9.6-7.2$m^3$/s, i.e. a decrease of about 45.1-58.9%.

Combination of statistical downscaling and stochastic analysis to generate daily series data together with a lump rainfall-runoff model can be used to simulate river discharge trends. However, the result may be unreliable for simulating extreme events. As shown in this study, the simulation result for very low flow tends to be overestimated, while the simulation result for average low flow or high flow for long time series may still produce a good result. Therefore, this type of analysis is suitable for projection of future water availability but not for extreme weather events.

The above analysis shows that the effect of climate change on river water discharge in the Upper CRB is clear. Therefore, the Upper CRB needs an appropriate land use policy, which restrains the increasing trend of land use change together with developing more alternatives for increasing the capacity of the water supply system and good flood management. Otherwise, more intense water resource problems will continue to emerge in the Upper CRB.

## Acknowledgement

This research was supported by the P3MI research scheme at the Institute of Technology Bandung.

## Referencess


[1] Kusuma, M.S.B, Kuntoro, A.A. & Silasari, R., *Preparedness Effort toward Climate Change Adaptation in Upper Citarum River Basin, West Java, Indonesia*, International Symposium on Social Management Systems, Kochi University, Japan, 2011.

[2] Nurcahyo, H., Soekarno, I., Hadihardaja, I.K. & Rosyidie, A., *Hydrologic Alteration in Watershed Using Flow Duration Curve, Case Study Upper Citarum Watershed, Indonesia*, International Proceedings of Chemical, Biological and Environment Engineering, Volume of IPCBEE, 2016.

[3] Julian, M.M., Nishio, F., Poerbandono & Ward, P.J., *Simulation of River Discharges in Major Watersheds or Northwestern Java from 1901 to 2006*, International Journal of Technology 1, pp. 37-46, 2011.

[4] Agaton, M., Setiawan, Y. & Effendi, H., *Land Use/Land Cover Change Detection in an Urban Watershed: A Case Study of Upper Citarum Watershed, West Java Province, Indonesia*, The 2nd International Symposium on LAPAN-IPB Satellite for Food Security and Environmental Monitoring 2015, LISAT-FSEM 2015, Procedia Environmental Sciences 33, pp. 654-660, 2016.

[5] Yoshida, K., Azechi, I., Hariya, R., Tanaka, K., Noda. K., Oki, K., Hongo, C., Honma, K., Maki, M. & Shirakawa, H., *Future Water Availability in the Asian Monsoon Region: A Case Study in Indonesia*, Journal of Developments in Sustainable Agriculture, **8**, pp. 25-31, 2013.

[6] Sahu, N., Yamashiki, Y., Takara, K. & Singh, R.B., *An Observation on the Relationship between Climate Variability Modes and River Discharge of The Citarum River Basin, Indonesia*, Annuals of Disas. Prev. Res. Inst., Kyoto Univ., **54B**, 2011.

[7] D'Arrigo, R. & Abram, N., *Reconstructed Streamflow for Citarum River, Java, Indonesia: Linkages to Tropical Climate Dynamics*, Clim Dyn, **36**, pp. 451-462, 2011.

[8] Kartiwa, B., Murniati E. & Burmodoi, A., *Application of Hydrological Model, RS and GIS for Flood Mapping of Citarum Watershed, West Java Province, Indonesia*, Journal of Remote Sensing Technology, **1**(1), pp. 1-8, 2013.

[9] KNMI Climate Explorer, https://climexp.knmi.nl. (accessed June 2017).

[10] Gutmann, E., Pruit, T., Clark, M.P., Brekke, L., Arnold, J.R., Raff, D.A. & Rasmussen, R.M. *An Intercomparison of Statistical Downscaling Methods used for Water Resource Assessments in the United States*, Water Resour. Res., 50, pp. 7167-7186, 2014.

[11] Hu, Y., Shreedhar, M. & Uhlenbrook, S., *Downscaling Daily Precipitation Over the Yellow River Source Region in China: a Comparison of Three Statistical Downscaling Methods,* Theor Appl Climatol, **112**, pp. 447-460, 2013.

[12] Hundecha, Y., Sunyer, M.A., Lawrence, D., Madsen, H., Willems, P., Bürger, G., Kriaučiūnienė, J., Athanasios, L., Martinkova, M., Osuch, M., Vasiliades, L., von Christierson, B., Vormoor, K. & Yücel, I., *Inter-Comparison of Statistical Downscaling Methods for Projection of Extreme Flow Indices across Europe*, Journal of Hydrology 541, pp. 1273-1286, 2016.

[13] Chen, H., Xu, C. & Guo, S., *Comparison and Evaluation of Multiple GCMs, Statistical Downscaling and Hydrological Models in the Study of Climate Change Impacts on Runoff*, Journal of Hydrology, **434–435**, pp. 36-45, 2012.

[14] Nyunt, C.T., Koike, T., Sanchez, P.A.J., Yamamoto, A., Nemoto, T. & Kitsuregawa, M,, *Bias Correction Method for Climate Change impact Assessment in the Philippines*, Journal of Japan Society of Civil Engineers, Ser.B1 (Hydraulic Engineering), **69**(4), I_19-I_24, 2013.

[15] Boland J.W. & Howlett, P., *Generating Synthetic Rainfall on Various Timescales – Daily, Monthly and Yearly*, Environmental Modelling and Assessment, DOI: 10.1007/s1066-008-9157-3, 2009.

[16] Rayner, D., Achberger, C. & Chen, D., *A Multi-state Weather Generator for Daily Precipitation for the Torne River Basin, Northern Sweden/western Finland*, Advances in Climate Change Research, **7**, pp. 70-81, 2016.

[17] Burnash, R.J.C, Feral, R.L. & McGuire, R.A., *A Generalized Streamflow Simulation System – Conceptual Modeling for Digital Computers*, U.S. Department of Commerce, National Weather Service and State of California, Department of Water Resources, 1973.

[18] Burnash, R.J.C., *The NWS River Forecast System – Catchment Modeling*, Computer Model of Watershed Hydrology, Singh, V.P, Water Resources Publication, pp. 311-366, 1995.

[19] Oyerinde, G.T. & Diekkrüger, B., *Influence of Parameter Sensitivity and Uncertainty on Projected Runoff in the Upper Niger Basin under a Changing Climate*, Climate, **5**(3), 67, 2017.

[20] Clanor, M.D.M., Escobar, E.C., Bondad, R.G.M., Duka, M.A., Ventura, J.R.S., Dorado, A.A., Lu, M.M.D., Sanchez, P.R.P. & Mulimbayan, F.M., *Daily Streamflow Forecasting of the Gauged Molawin Watershed Using Model Combinations and the Ungauged Eastern Dampalit Watershed by Spatial Proximity Regionalization*, Philippine e-Journal for Applied Research and Development, **6**, pp. 19-31, 2016.

[21] Newman, A.J., Clark, M.P., Sampson K., Wood, A., Hay, L.E., Bock, A., Viger, R.J, Blodgett, D., Brekke, L., Arnold, J.R., Hopson, T. & Duan Q., *Development of a Large-sample Watershed-scale Hydrometeorological Data Set for the Contiguous USA: Data Set Characteristics and*

*Assessment of Regional Variability in Hydrologic Model Performance*, Hydrol. Earth Syst. Sci., **19**, pp. 209-223, 2015.

[22] Krause, P., Boyle, D.P. & Base, F., *Comparison of Different Efficiency Criteria For Hydrological Model Assessment*, Advances in Geosciences, European Geosciences Union, 2005.